Supporting Information

# Bioprinted Injectable Hierarchically Porous Gelatin Methacryloyl Hydrogel Constructs with Shape-Memory Properties

*Guoliang Ying*, *Nan Jiang*, *Carolina Parra*, *Guosheng Tang*, *Jingyi Zhang*, *Hongjun Wang, Shixuan Chen, Ning-Ping Huang*, *Jingwei Xie, and Yu Shrike Zhang**

Dr. G. Y., C. P., G. T., J. Z., Prof. Y. S. Z.

Division of Engineering in Medicine, Department of Medicine, Brigham and Women's Hospital, Harvard Medical School, Cambridge, MA 02139, USA

E-mail: yszhang@research.bwh.harvard.edu

Dr. N. J.

School of Engineering and Applied Sciences, Harvard University, Cambridge, MA 02138, USA

J. Z., Prof. N.-P. H.

State Key Laboratory of Bioelectronics, School of Biological Science and Medical Engineering, Southeast University, Nanjing 210096, China

H. W., S. C., Prof. J. X.

Department of Surgery-Transplant and Holland Regenerative Medicine Program University of Nebraska Medical Center, Omaha, NE 68198, USA

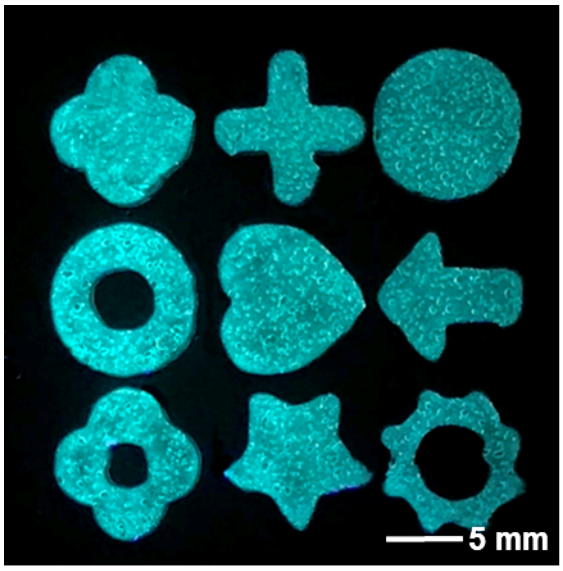


**Fig. S1.** Top-view photograph of the 3D-bioprinted micro-nanoporous GelMA hydrogel constructs under UV light illumination.

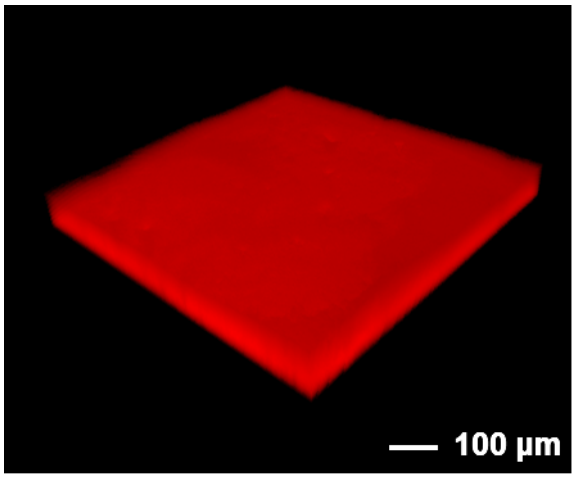


**Fig. S2.** Confocal 3D re-construction of a standard hydrogel construct.

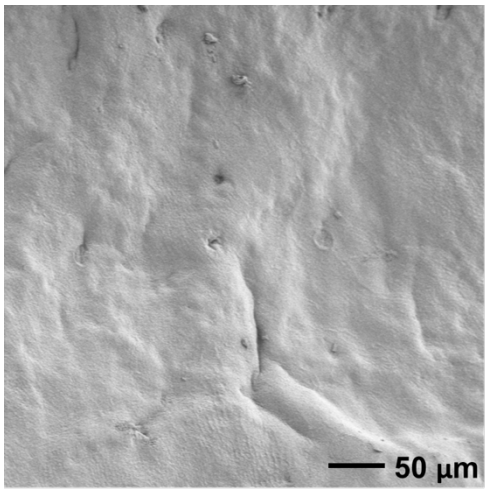


**Fig. S3.** SEM micrograph of a standard GelMA hydrogel.

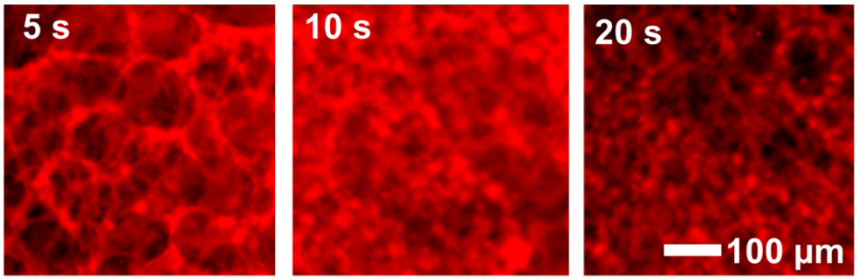


**Fig. S4.** Fluorescence micrographs showing the porous GelMA hydrogel constructs (PEO: 50 vol%) at mixing time of (i) 5 s, (ii) 10 s, and (iii) 20 s.

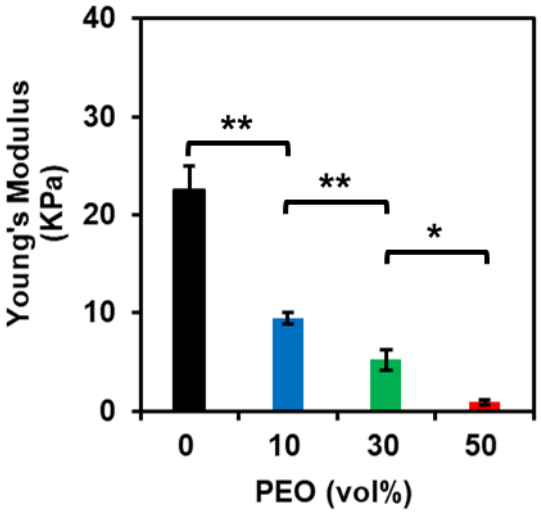


**Fig. S5.** Young's Moduli of hydrogel constructs as a function of PEO volume fraction. Error bars represent standard deviations (n=3, *$p$<0.05, **$p$<0.01).

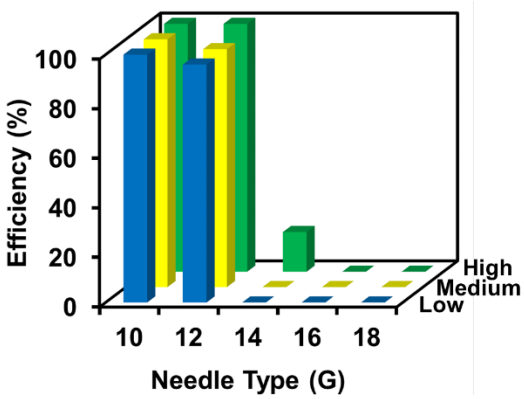


**Fig. S6.** Injectability evaluations of the 3D-bioprinted standard hydrogel constructs using various gauges of percutaneous needles.

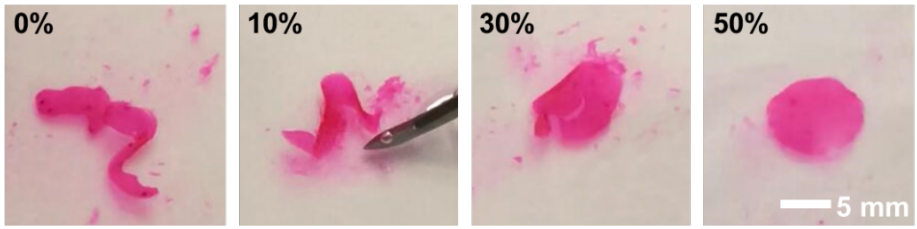


**Fig. S7.** Photographs of the 3D-bioprinted micro-nanoporous hydrogel constructs (without the macropores) at different PEO volume fractions after injection through a 14G percutaneous needle.

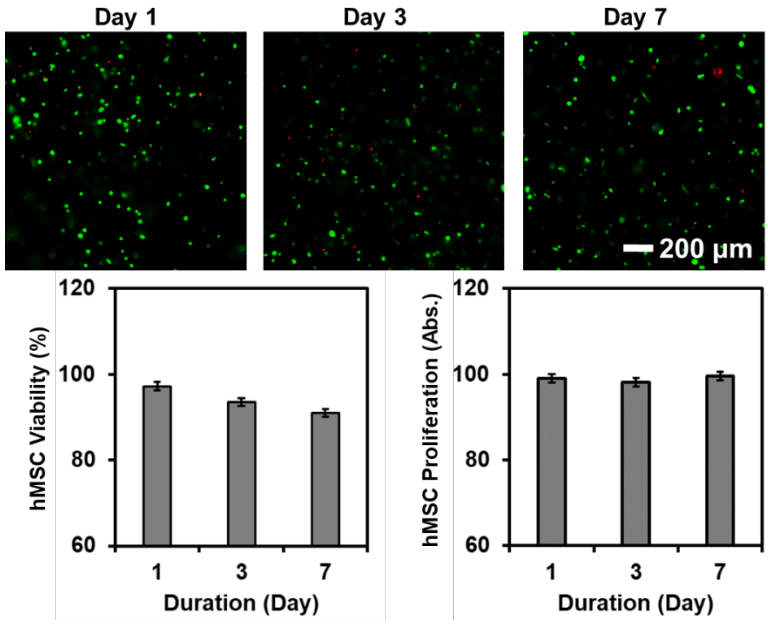


**Fig. S8.** Evaluations of cell viability and proliferation in standard hydrogel constructs. Error bars represent standard deviations (n=3).

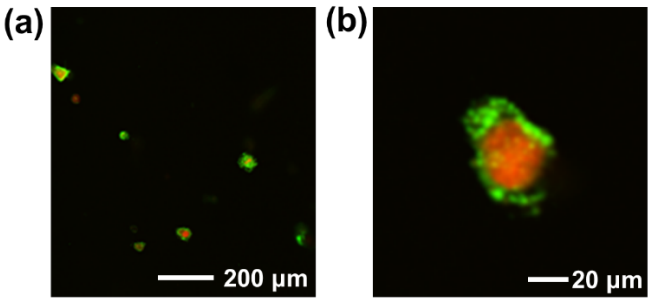


**Fig. S9.** (a) Fluorescence micrographs of hMSCs spreading within a standard GelMA hydrogel construct. (b) Magnified image showing a single hMSC. The cells were stained for F-actin (green) and nuclei (red).

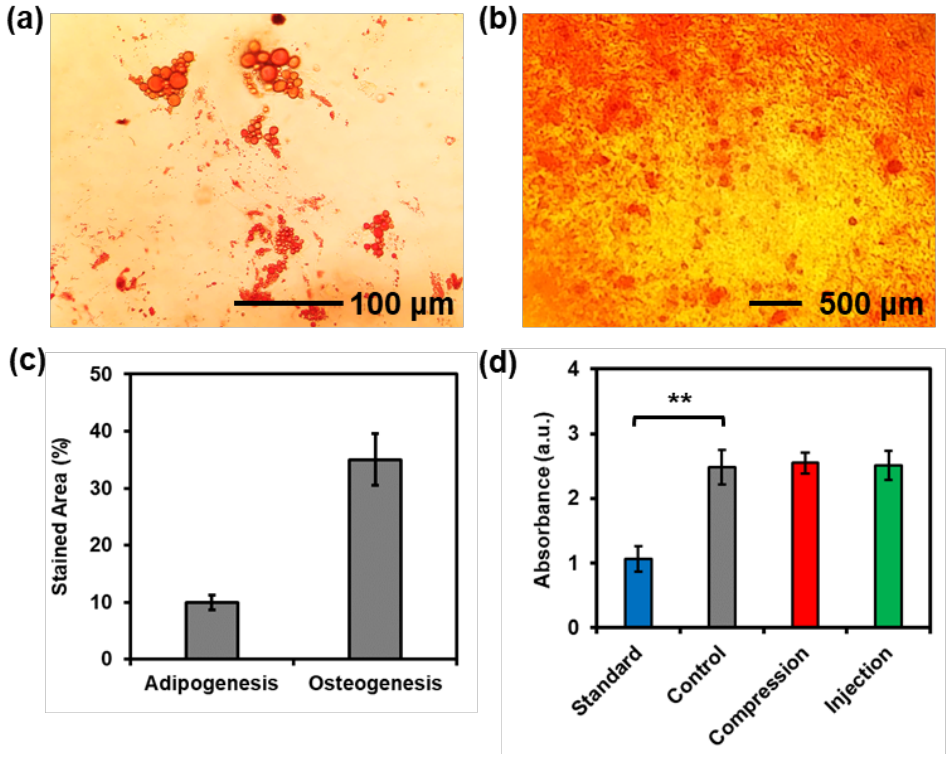


**Fig. S10.** Bright-field micrographs of 3-week differentiated hMSCs stained with (a) Oil Red O (for adipogenesis) and (b) Alizarin Red S (for osteogenesis). (c) Semi-quantitative measurements of adipogenesis and osteogenesis. (d) Densitometric analyses of Alizarin Red S staining to quantify the osteogenic differentiation. Error bars represent standard deviations (n=3, $^{**}p<0.01$).

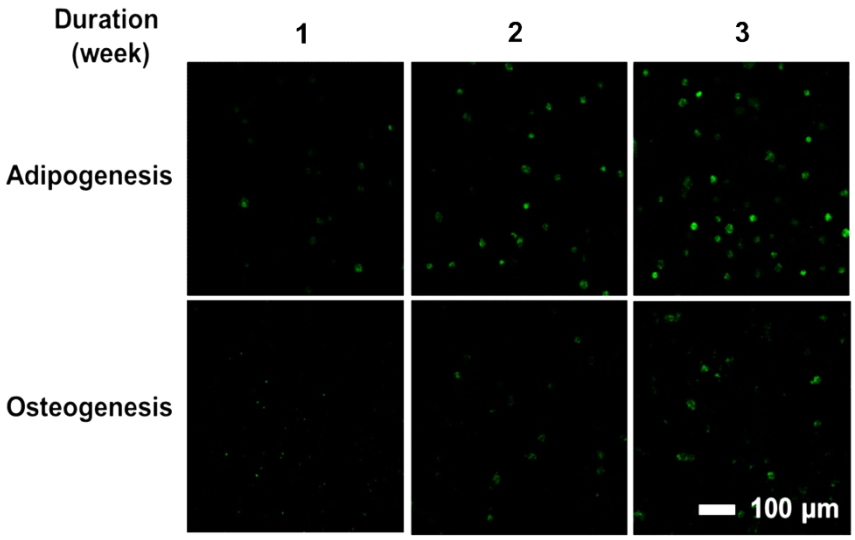


**Fig. S11.** Fluorescence micrographs of immunostained, differentiated hMSCs in the standard hydrogel constructs. For adipogenesis, hMSCs were stained for PPARγ. For osteogenesis, hMSCs were stained for RUNX2.

**Table S1.** Evaluation of the effects of syringe needle gauge and methacryloyl substitution on injectability (n=25 in each group).

| | Needle gauge | Inner diameter (mm) | Outer diameter (mm) | Passage efficiency (control) (%) | Passage efficiency (hierarchically porous) (%) |
|---|---|---|---|---|---|
| **Low degree of substitution** | 10 | 2.69 | 3.40 | 100 | 100 |
| | 12 | 2.16 | 2.77 | 96 | 100 |
| | 14 | 1.45 | 1.82 | 0 | 60 |
| | 16 | 1.32 | 1.60 | 0 | 12 |
| | 18 | 0.90 | 1.26 | 0 | 0 |
| **Medium degree of substitution** | 10 | 2.69 | 3.40 | 100 | 100 |
| | 12 | 2.16 | 2.77 | 96 | 100 |
| | 14 | 1.45 | 1.82 | 0 | 88 |
| | 16 | 1.32 | 1.60 | 0 | 24 |
| | 18 | 0.90 | 1.26 | 0 | 0 |
| **High degree of substitution** | 10 | 2.69 | 3.40 | 100 | 100 |
| | 12 | 2.16 | 2.77 | 100 | 100 |
| | 14 | 1.45 | 1.82 | 16 | 96 |
| | 16 | 1.32 | 1.60 | 00 | 40 |
| | 18 | 0.90 | 1.26 | 0 | 0 |

**Table S2.** Evaluation of the effect of methacryloyl substitution on injectability using 14G needle (n=25 in each group).

| Needle gauge | Inner diameter (mm) | Outer diameter (mm) | Passage efficiency (%) (low) | Passage efficiency (%) (medium) | Passage efficiency (%) (high) |
|---|---|---|---|---|---|
| **14G** | 1.45 | 1.82 | 60 | 88 | 96 |

**Movie S1 (separate file).** Video of the 3D bioprinting process of the micro-nanoporous GelMA hydrogel constructs.

**Movie S2 (separate file).** Video of compression test of a standard GelMA hydrogel construct. The hydrogel construct stained in blue, was sandwiched between two clear pressure pads. After a single compression, the shape and structure of hydrogel construct were damaged.

**Movie S3 (separate file).** Video of compression test of a micro-nanoporous GelMA hydrogel construct. The hydrogel construct stained in blue, was sandwiched between two clear pressure pads. After several compression cycles, the hydrogel construct kept its original shape and structure without being damaged.

**Movie S4 (separate file).** Video of injection of a hierarchically porous GelMA hydrogel construct produced from the bioink with 10 vol% PEO. The hydrogel construct stained in blue, was injected through a 14G percutaneous needle. After a single injection, the hydrogel construct was collapsed.

**Movie S5 (separate file).** Video of injection of a hierarchically porous GelMA hydrogel construct produced from the bioink with 30 vol% PEO. The hydrogel construct stained in blue, was injected through a 14G percutaneous needle. After a single injection, the hydrogel construct readily recovered to its original shape.

**Movie S6 (separate file).** Video of injection of a hierarchically porous GelMA hydrogel construct produced from the bioink with 50 vol% PEO. The hydrogel construct stained in blue,

was injected through a 14G percutaneous needle. After a single injection, the hydrogel construct readily recovered to its original shape.

**Movie S7 (separate file).** Video of injection of a standard GelMA hydrogel construct. The hydrogel construct stained in blue, was injected through a 14G percutaneous needle. After a single injection, the hydrogel construct collapsed.

**Movie S8 (separate file).** Video of *ex vivo* injection of a shape-memory hierarchically porous GelMA hydrogel construct. The hydrogel construct stained in blue, was injected into the defect within a porcine tissue through a 14G percutaneous needle. After syringe injection, the hydrogel construct was observed to promptly recover to the original shape, which precisely fit the defect in the porcine tissue.

**Movie S9 (separate file).** Fluorescence video of 3D re-construction of hMSC spreading within a hierarchically porous hydrogel construct.

**Movie S10 (separate file).** Fluorescence video of 3D re-construction of hMSC spreading within a standard hydrogel construct.